

Supplementary information

Nanohybrid Biosensor Based on Mussel-Inspired Electro-crosslinking of Tannic Acid Capped Gold Nanoparticles and Enzymes

Rémy Savin,^a Nour-Ouda Benzaamia,^a Christian Njel,^b Sergey Pronkin,^c Christian Blanck,^a
Marc Schmutz,^a Fouzia Boulmedais^{a,d*}

a. Université de Strasbourg, CNRS, Institut Charles Sadron UPR 22, 67034 Strasbourg, France.

b. Institute for Applied Materials (IAM) and Karlsruhe Nano Micro Facility (KNMF), Karlsruhe Institute of Technology (KIT), D-76344 Eggenstein-Leopoldshafen, Germany

c. Université de Strasbourg, CNRS, ICPEES UMR 7515, 67087 Strasbourg, France.

d. International Center for Frontier Research in Chemistry, 67083 Strasbourg, France.

S1 – Enzyme characterization

The batches of enzymes were characterized as follows regarding the content in protein and their activity. The enzyme concentration was determined from tryptophan, tyrosine and cysteine residues using the absorbance value at 280 nm and the cofactor absorbance using the extinction coefficients (Table S1). The Bradford test was also performed to determine the concentration in protein using the ready-to-use methanol/coomassie Blue solution from Sigma-Aldrich (B6916). A calibration curve was prepared with bovine serum albumin (BSA) using 5 μL of this standard enzyme solution with concentration ranging from 0.1 to 1.4 $\text{mg}\cdot\text{mL}^{-1}$. 250 μL of undiluted B6916 solution was then added to the enzyme solution, solution was stirred and the absorbance at 595 nm was recorded after 45 min. Color change from 465 nm (cationic brown/red, unbound dye) to (anionic blue, bound dye) arises from the formation of a non-covalent complex with carboxyl and amino group of proteins.

Table S1: Extinction Coefficient of the enzymes used in the study

Enzyme	GOx	HRP
Wavelength (nm)	280	280
Extinction Coefficient ($\text{mM}^{-1}\cdot\text{cm}^{-1}$)	263 ¹	19.6 ²

Table S2: Content in enzyme

Enzyme	Enzyme content according to			
	Provider	Bradford test	Absorbance at 280 nm	Value used in the study
GOx	78 - 81%	76 \pm 4%	74 \pm 2%	80%
HRP	Not specified	90 \pm 7 %	91.1 \pm 0.3 %	90%

S2 – Theoretical molar ratio of GOx/TA@AuNPs of an adsorbed monolayer

Knowing the TA@AuNPs size (12 nm) and GOx size (7 nm), the number of enzymes, considered as a rigid sphere, covering the TA@AuNPs as monolayer was determined using the following equation. First, the surface of coverage was determined using the radius of NPs and GOx ($R_{\text{NP}} + R_{\text{GOx}}$) with $S_{\text{coverage}} = 4 \times \pi \times (R_{\text{NP}} + R_{\text{GOx}})^2$ and the footprint of the

enzyme was supposed to be: $S_{GOx} = \pi \times R_{GOx}^2$. Then, the GOx/NP molar ratio – without compacity factor, was determined as: $R = \frac{4 \times (R_{NP} + R_{GOx})^2}{R_{GOx}^2}$

S3 - Stability of TA@AuNPs suspension during the storage

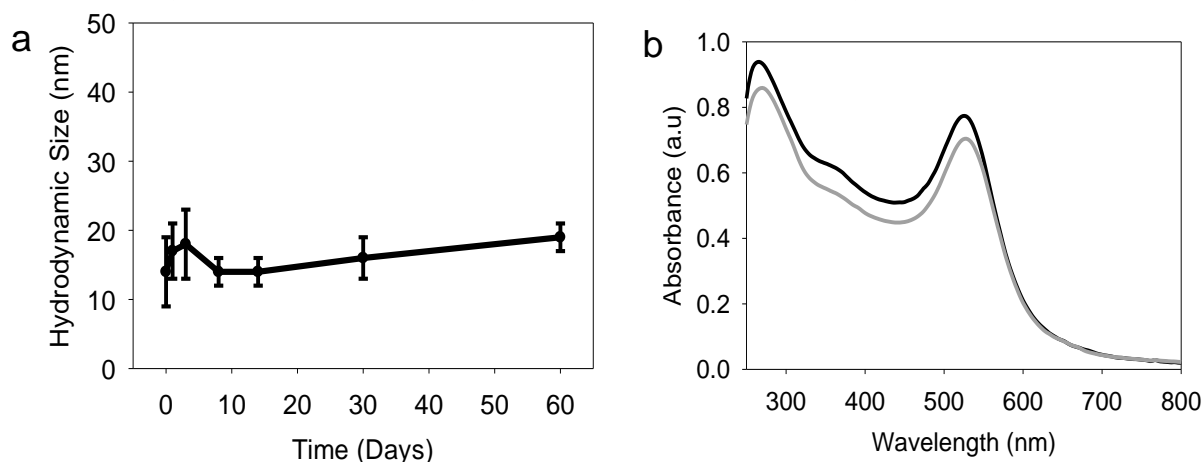


Fig. S1 TA@AuNPs suspension: (a) Hydrodynamic size, measured in intensity by DLS, at different time upon storage at 4°C under argon, (b) Absorbance spectra after one day (black) and after two month of storage (grey).

S4 - Size of Aggregation test

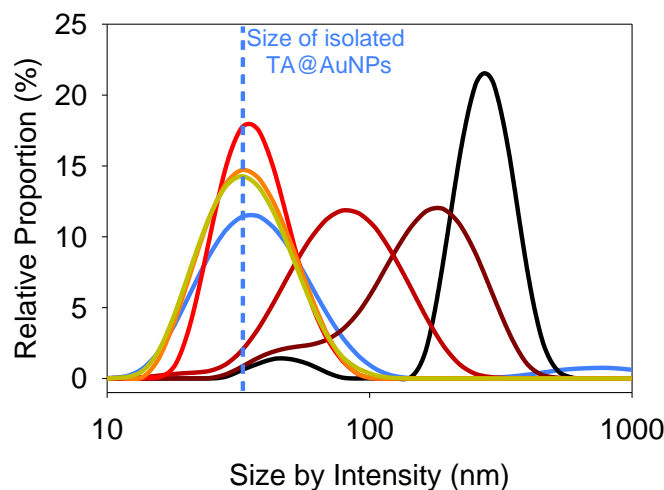


Fig. S2 Hydrodynamic size, measured in intensity by DLS, of TA@AuNPs in water (blue) and GOx/TA@AuNPs suspensions in the presence of 1 M NaCl, as a function of the GOx/NP molar ratio at 0 (black), 6.7 (brown), 13.4 (dark red), 34 (red), 67 (orange), 140 (yellow).

S5 – Enzymatic inhibition of GOx in the presence of TA and TA@AuNPs

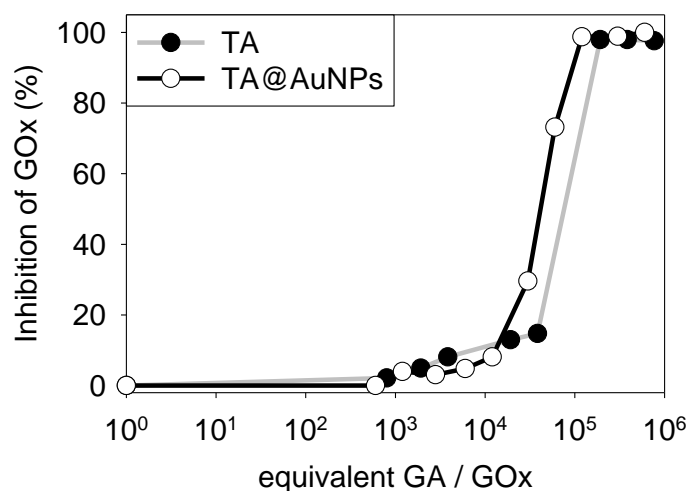


Fig. S3 GOx/TA solution and GOx/TA@AuNPs suspension activity: GOx enzymatic inhibition in the presence of TA and TA@AuNPs as a function of the molar ratio in equivalent GA moieties/GOx.

S6 – Bare gold QCM crystal and TA@AuNPs coating

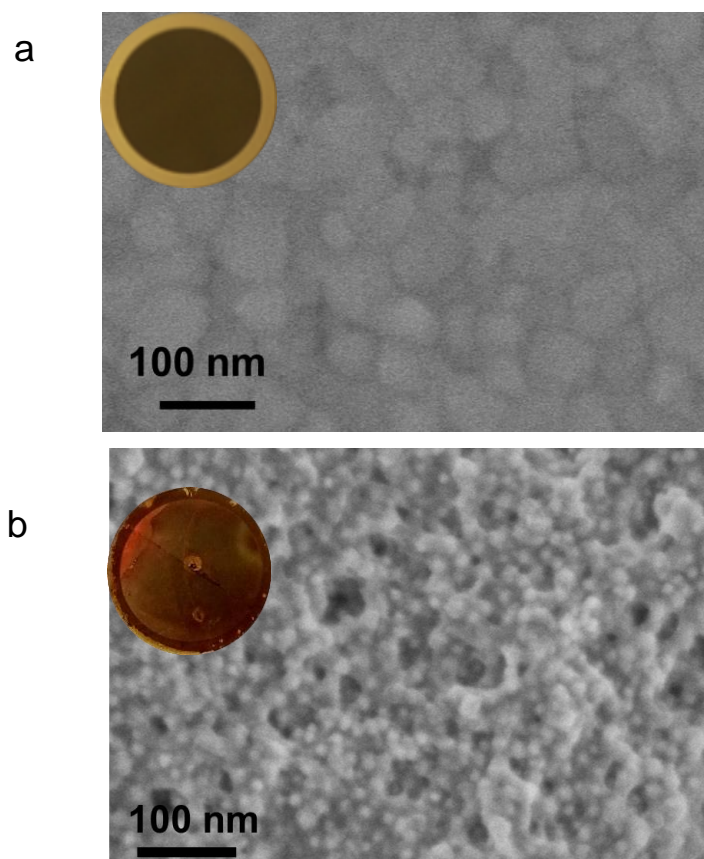


Fig. S4 Pictures and SEM micrographs, with secondary electron detector of (a) a bare gold QCM crystal and (b) with TA@AuNPs coating, obtained by electro-crosslinking of FcOH/TA@AuNPs mixture on gold QCM crystal.

S7 – XPS survey of dropcasted and electrodeposited samples

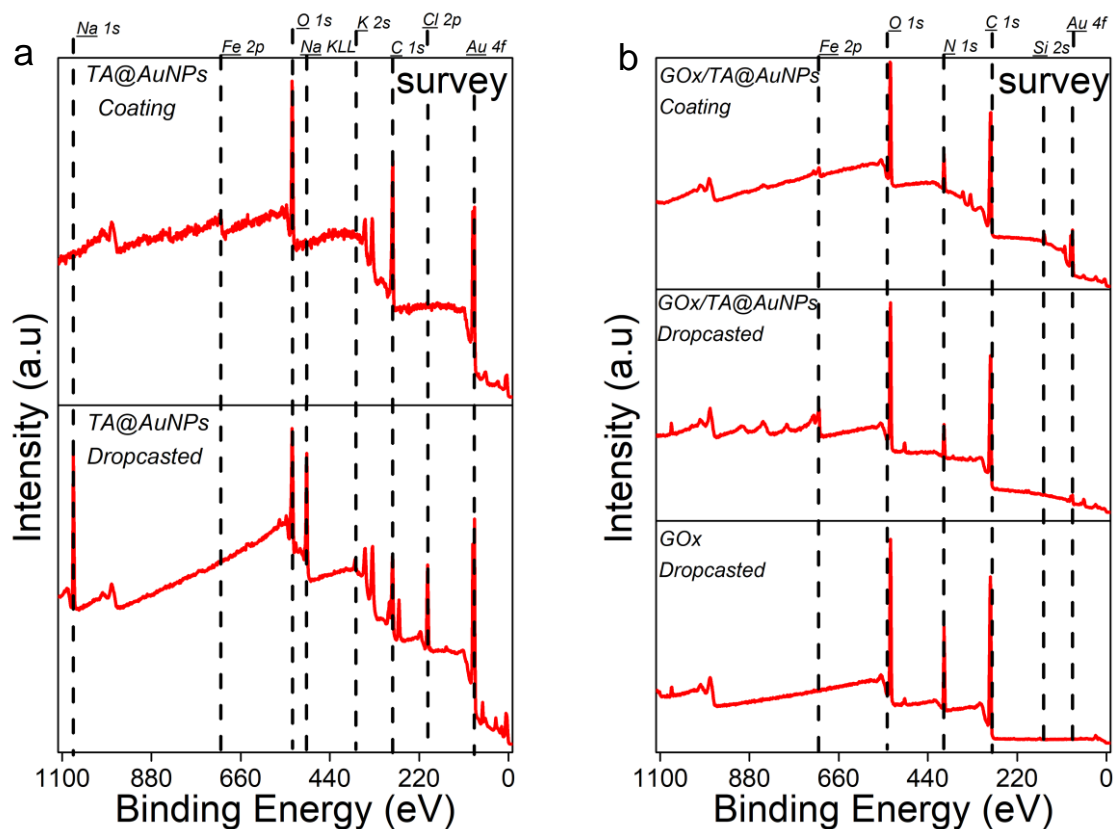


Fig. S5 XPS survey spectra of (a) TA@AuNPs coating, obtained by electrodeposition of FcOH/TA@AuNPs and TA@AuNPs dropcasted solution, (b) GOx/TA@AuNPs coating, obtained by electrodeposition of FcOH/GOx/TA@AuNPs, FcOH/GOx/TA@AuNPs solution and GOx solution dropcasted

S8 – Electrocatalytic current of glucose biosensor in cyclic voltammetry and with chronoamperometry at 0.25V

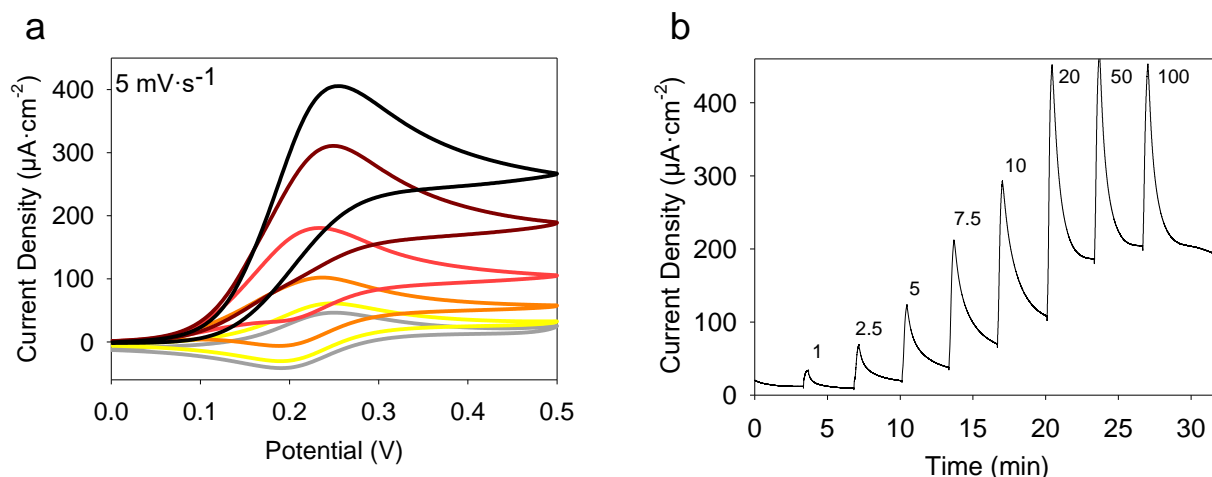


Fig. S6 (a) Cyclic voltammograms, performed at a scan rate of 5 mV s^{-1} , of GOx/TA@AuNPs coating in contact with $0.5\text{ mM FcOH}/10\text{ mM PBS}$ solution, containing 0 (grey), 1 (yellow), 2.5 (orange), 5 (red), 10 (brown) and 50 mM (black) of glucose. (b) Chronoamperometric curve, measured at 0.25 V , of GOx/TA@AuNPs coating upon addition of different concentration of glucose solution, prepared in $0.5\text{ mM FcOH}/10\text{ mM PBS}$, ranging from 1 to 100 mM .

S9 – Influence of Tween-20 test on glucose biosensor

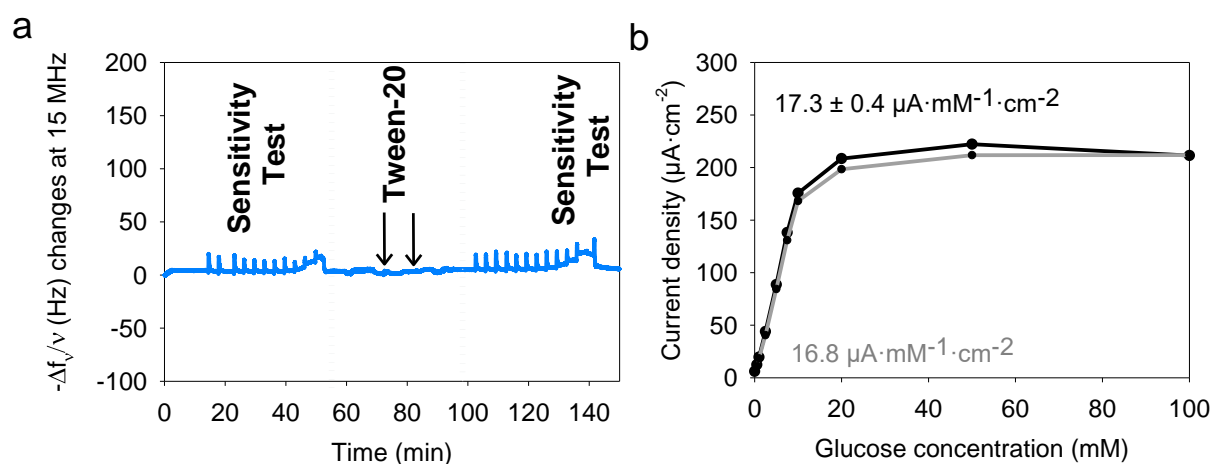


Fig. S7 Tween-20 treatment of GOx/TA@AuNPs coating (a) Evolution of the normalized frequency shift, measured by QCM-D, as a function of time before and after addition of Tween-20 0.01% (b) Current density, measured at 0.25 V in the presence of $0.5\text{ mM FcOH}/10\text{ mM PBS}$, as function of glucose concentration, before (black curve) and after (grey curve) Tween-20 treatment.

S10 – Glucose biosensor stability upon storage at room temperature

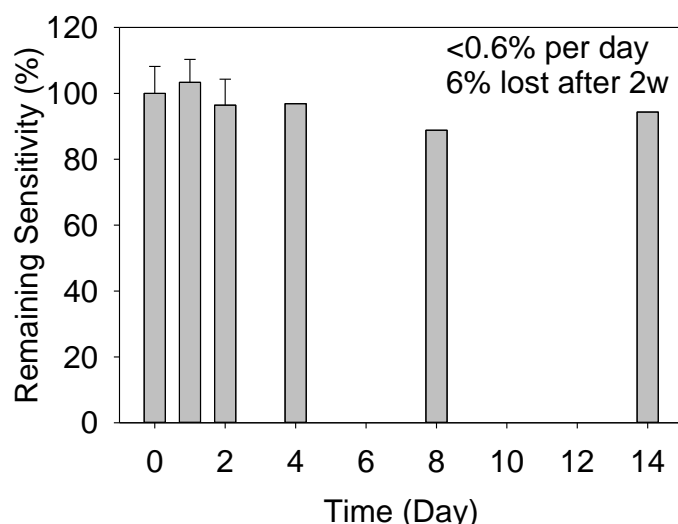


Fig. S8 Sensitivity of GOx/TA@AuNPs coating, measured from chronoamperometric experiments at different days upon storage in 10 mM PBS at room temperature in the QCM cell.

S11 – Glucose response time and sensitivity of GOx/TA@AuNPs on 10 μ m- Au array electrode

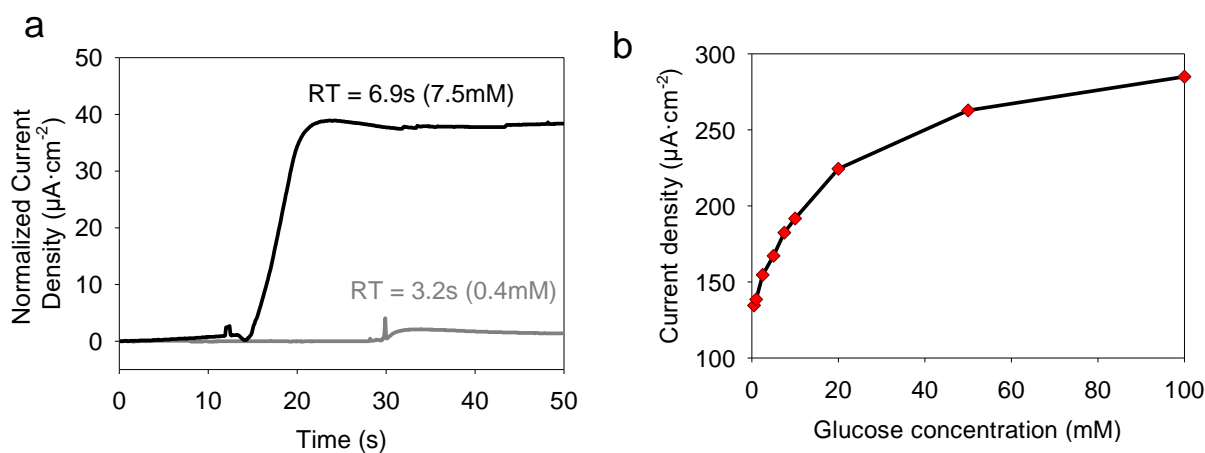


Fig. S9 GOx/TA@AuNPs coating electrodeposited on 10- μ m-Au array electrode: (a) Response time at 0.25 V at 0.4 (grey curve) and 7.5 (black curve) mM of glucose. The measurement was performed by addition of 10 μ L, i.e. 0.4 mM and 200 μ L, i.e. 7.5 mM of glucose solution (100 mM glucose/0.5 mM FcOH/10 mM PBS) into 2.5 mL 0.5 mM FcOH/10 mM PBS. (b) Current density, measured at 0.25 V and 20 s after glucose addition, as function of the glucose concentration.

- (1) Courjean, O.; Flexer, V.; PrévotEAU, A.; Suraniti, E.; Mano, N. Effect of Degree of Glycosylation on Charge of Glucose Oxidase and Redox Hydrogel Catalytic Efficiency. *ChemPhysChem* **2010**, *11*, 2795–2797.
- (2) Strickland, E. H.; Kay, E.; Shannon, L. M.; Horwitz, J. Peroxidase Isoenzymes from Horseradish Roots: III. Circular Dichroism of Isoenzymes and Apoisoenzymes. *J. Biol. Chem.* **1968**, *243* (13), 3560–3565.